PLOS ONE

Streptococcus pneumoniae serotype 22F infection in respiratory syncytial virus infected neonatal lambs enhances morbidity

Sarhad Alnajjar[1,2,3]**, Panchan Sitthicharoenchai**[1]**, Jack Gallup**[1]**, Mark Ackermann**[3]**, David Verhoeven**[ID][4]*

1 Department of Veterinary Pathology, College of Veterinary Medicine, Iowa State University, Ames, Iowa, United States of America, **2** Department of Veterinary Pathology, College of Veterinary Medicine, Baghdad University, Baghdad, Iraq, **3** Department of Biomedical Sciences, Carlson College of Veterinary Medicine, Oregon State University, Corvallis, Oregon, United States of America, **4** Department of Veterinary Microbiology and Preventative Medicine, College of Veterinary Medicine, Iowa State University, Ames, Iowa, United States of America

* davidver@iastate.edu

Abstract

Respiratory syncytial virus (RSV) is the primary cause of viral bronchiolitis resulting in hospitalization and a frequent cause of secondary respiratory bacterial infection, especially by *Streptococcus pneumoniae (Spn)* in infants. While murine studies have demonstrated enhanced morbidity during a viral/bacterial co-infection, human meta-studies have conflicting results. Moreover, little knowledge about the pathogenesis of emerging *Spn* serotype 22F, especially the co-pathologies between RSV and *Spn*, is known. Here, colostrum-deprived neonate lambs were divided into four groups. Two of the groups were nebulized with RSV M37, and the other two groups were mock nebulized. At day three post-RSV infection, one RSV group (RSV/*Spn)* and one mock-nebulized group (*Spn only*) were inoculated with *Spn* intratracheally. At day six post-RSV infection, bacterial/viral loads were assessed along with histopathology and correlated with clinical symptoms. Lambs dually infected with RSV/*Spn* trended with higher RSV titers, but lower *Spn.* Additionally, lung lesions were observed to be more frequent in the RSV/*Spn* group characterized by increased interalveolar wall thickness accompanied by neutrophil and lymphocyte infiltration and higher myeloperoxidase. Despite lower *Spn* in lungs, co-infected lambs had more significant morbidity and histopathology, which correlated with a different cytokine response. Thus, enhanced disease severity during dual infection may be due to lesion development and altered immune responses rather than bacterial counts.

Introduction

Respiratory Syncytial Virus (RSV) is one of the leading causes of severe lower respiratory infection in infants under the age of five, leading to 600,000 yearly deaths worldwide [1]. RSV is a member of the pneumoviridae family that infects most infants by the age of two years [2].

Although a mild to moderate upper respiratory tract infection is the most common form of infection, severe lower respiratory tract infections can develop, leading to bronchiolitis that frequently necessitates hospitalization and sometimes causes death [3]. Lower respiratory tract infections can also increase the susceptibility to secondary bacterial infection(s), leading to severe and life-threatening pneumonia [4]. *Streptococcus pneumoniae* (*Spn*) is one of the most common bacterial infections that occur concurrently with respiratory viruses such as influenza and RSV [5, 6], but unlike influenza, less is known about common etiologies during a dual RSV/*Spn* infection. While secondary bacterial pneumonia is well known for influenza, clinical data suggests RSV can also often cause bacterial pneumonia that is not well recognized. Moreover, RSV is associated with invasive *Spn* such as pneumonia in the young or immunocompromised [7–11]. Other studies have also demonstrated that RSV is the most significant cause of pneumonia in infants with *Spn* co-infection very common [12–14]. However, the mechanisms associated with secondary *Spn* pneumonia in RSV infected children are not well known.

Spn is a Gram-positive facultative anaerobic bacterial pathogen that causes invasive diseases, including sepsis, meningitis, and pneumonia [15]. Like RSV, *Spn* causes severe illness and presents a higher incidence in both children and the elderly worldwide [16]. Pneumococcal pneumonia is one of the leading causes of bacterial pneumonia in children worldwide, responsible for about 11% of all deaths in children under the age of five (700,000–1 million every year). Most of these deaths occur in developing countries [17]. While *Spn* vaccines are effective in reducing the incidence of pneumonia caused by the serotypes contained in the vaccine [18], the emergence of non-vaccine serotypes, and persistence of antibiotic-resistant *Spn*, such as serotype 19A, highlights the importance of more investigation into *Spn* pathogenesis and therapy. Since *Spn* plays an essential role in secondary bacterial infections following viral pneumonia or viral-bacterial co-infection [16, 19], animal modeling for understanding viral-bacterial co-infections is crucial to investigating therapeutics that combat both.

Most prior studies have concentrated on influenza and *Spn* co-infections and mainly in murine models. Few mechanistic studies have been done in humans other than the calculation of frequencies of co-infections with these two pathogens [20–22]. Importantly, despite the importance of RSV/*Spn* co-infections, far fewer studies in this area as compared to influenza/ *Spn* have been done, which may relate partially to difficulties of using RSV in animal models such as mice [23–25]. Furthermore, less is known about emergent serotype 22F pathogenesis [19, 26]. 22F infections have risen with time, with one study showing an annual incidence rate of 0.5 per 411 samplings in 2000–2001 that increased to 10% of samples in 2005–2007 [26]. In a more recent study, serotype 22F was the most common non-PCV13 [27] strain found in children with invasive disease [28]. Furthermore, serotype 22F was more virulent than emerging serotype 33F (the third most common non-PCV13 in children), and capsule transfer to a laboratory strain increased that strain's ability to replicate in the blood of challenged mice. 22F was also found to be more lethal in mice than 33F in that same study [28]. How this bacterial serotype behaves in conjunction with a concurrent respiratory viral infection is not yet known.

We have extensively used a neonatal lamb model to mimic RSV lower respiratory tract infection in infants as a preclinical model to evaluate the efficacy of new therapeutics [29] and to understand RSV pathogenesis [30–32]. Sheep are also permissive to *Spn* infection and have served as an *Spn* sepsis model that appears to manifest clinical signs similar to human infection [33, 34]. Thus, our current study had a few objectives: (1) Can we model RSV/*Spn* pneumonia in a large infant animal species that can be improved in future studies; (2) can we successfully dually infect lambs and do we get enhanced disease; (3) can we use the model to gain insights into mechanisms that enhance morbidity over the single pathogen control groups; and (4) can we use infant lambs to study *Spn* pathogenesis? A minor goal was also to determine whether we could get bacterial pneumonia without sepsis that is common in murine studies but not

human infections. We hypothesized, based mostly on influenza dual infections, that RSV and *Spn* infected lambs would exhibit higher viral and/or bacterial burdens when dually infected. However, here, we determined that pathogen burdens did not correlate with levels of viral lesions or bacterial burdens but rather with different tissue damage and immune responses between groups.

Material and methods

Experimental design

Animals. A total of 20, 2–3 day-old, colostrum-deprived lambs, were randomly divided into four groups with five animals per group: RSV only, RSV-Spn co-infection, Spn only, and uninfected control. Animals were group-housed by experimental groups to reduce stress and colostrum as withheld to reduce any interference with cross-reactive anti-ovine RSV immune responses passing to the lamb. W*e* do not envision that this would alter their immune responses to the virus. RSV, *Spn*, and uninfected controls were held in separate rooms. This study was carried out in strict accordance with the recommendations in the Guide for the Care and Use of Laboratory Animals and the USDA. Animal use was approved by the Institutional Animal Care and Use Committee of Iowa State University. All experiments were performed following relevant guidelines and regulations as set by regulatory bodies.

Infectious agents. Lambs were infected with RSV strain M37, purchased from Meridian BioSciences (Memphis, TN, USA). This strain is a wild type A RSV isolated from the respiratory secretions of an infant hospitalized for bronchiolitis [35, 36]. M37 was grown in HELA cells and stored at -80°C in media containing 20% sucrose [37]. 6 mL of 1.27×10^7 IFFU/mL in media containing 20% sucrose or cell-conditioned mock media (also containing 20% sucrose) was nebulized using PARI LC Sprint™ nebulizers to each lamb over 25–30 minutes resulting in the total inhalation of about 3 mL by each lamb [37]. *Spn* serotype 22F was grown overnight at 37°C in Todd Hewitt media containing 2% yeast extract, 50 μg/ml of gentamicin, and 10% bovine serum. Colony-forming units (CFUs) were calculated by OD_{600} with confirmation by dilution plating on Tryptic Soy Agar (TSA) plates with 5% sheep blood containing gentamicin.

Infections. For viral inoculations, infectious focus forming units (IFFU), where only replication-competent virus is detected by antibody in limiting dilution assays, were utilized. Two groups were exposed to nebulized RSV M37 (1.27×10^7 IFFU/mL), as done previously [37, 38], on day 0. One of the RSV infected groups was inoculated intratracheally with 2 ml normal saline as a mock Spn infection (RSV group) using syringe and needle, while the second RSV-infected group was inoculated intratracheally with 2 ml solution containing Spn serotype 22F (2×10^6 CFU/ml) 3 days post-RSV nebulization (RSV-Spn group). The other two groups were exposed to nebulized cell-conditioned mock media containing 20% sucrose at day 0 and inoculated intratracheally with either normal saline (control group) or solution containing Spn (2×10^6 CFU/ml) at day three post nebulization (Spn group). At day six post-RSV infection, all lambs were humanely euthanized with Fatal Plus immediately before necropsy.

Gross pathology. An autopsy was performed to evaluate the macroscopic lung lesions. After removal, each lung was examined by a pathologist similar to prior studies [38, 39]. If lesions were present, percentage involvement was estimated for each lung lobe. Percentages were converted to a scale using the following formula: 0% = 0, 1–9% = 1, 10–39% = 2, 40–69% = 3, 70–100% = 4. Group averages were calculated for the gross lesion score. Lung samples were collected, including sterile lung tissue for bacterial isolation, frozen lung sample for RT-qPCR, bronchioalveolar lavage fluid (BALF) from right caudal lung lobe for RSV IFFU assay and RT-qPCR, and lung pieces from different lobes were fixed in 10% neutral buffered formalin for histological assessment.

Clinical observations. Animals were observed three times daily and scored (1–5 on severity) by blinded animal caretakers concerning clinical symptoms including wheezing, lethargy, coughing, nasal/eye discharge while also taking a daily rectal temperature. The animal caretakers were all experienced with RSV infections in lambs from prior studies; however, this was the first time this scoring system has been used. The specific end-point for the study was six days post-RSV infection or if an animal appeared in respiratory distress, failed to take milk replacement at feeding times for longer than 24 hours, or were lethargic. Two animals were euthanized during the study before the six days after meeting the above-stated end-points due to sepsis.

Lung RSV viral and *Spn* bacterial titers. BALF collected from the right caudal lobe at necropsy by flushing the caudal lobe with 5 mL of cold DMIM and collected back several times as done previously [37, 38]. Collected BALF was used to evaluate RSV IFFU (Plaque assay that counts the number of syncytial cells formed due to viral infection detected by fluid fluorescent antibody technique). BALF was spun for 5 minutes at 3,000g to pellet large debris. Supernatants were spun through 0.45 am Costar SPIN-X filters (microcentrifuge 15,600g) for 5 minutes. The resulting BALF samples were applied to HELA cells grown to 70% confluence in 12-well culture plates (Fisher Scientific, Hanover Park, IL) at full strength, and three serial dilutions (1:10, 1:100, and 1:1000); all samples were tested in triplicate to determine the viral titer. Plates were stained with a fluorescent antibody technique and as described previously [37, 38]. 100 μL of the right caudal lobe BALF was added to 1 mL Trizol (Invitrogen) and kept at −80°C for the qRT-PCR assay to assess RSV mRNA. Sterile lung tissue samples were used to determine *Spn* titer. Lung tissue samples were placed in 500 μl of sterile PBS and were mechanically homogenized by a pestle. Lung homogenates were pelleted at 100g, for 5 minutes. Supernatants were serially diluted and applied to 5% sheep blood TSA plates containing gentamycin.

Immunohistochemistry (IHC). Formalin-fixed paraffin-embedded tissue sections were used for IHC, which was performed according to a previously published protocol in our laboratory [32, 37]. Briefly, after deparaffinization and rehydration, antigen retrieval was performed in 10mM TRIZMA base (pH 9.0), 1mM EDTA buffer, and 0.05% Tween 20 with boiling under pressure for up to 15 minutes. Polyclonal goat anti-RSV antibody (Millipore/Chemicon, Temecula, CA; Cat. No. AB1128) was used as the primary antibody after two blocking steps. The first blocking was with 3% bovine serum albumin in Tris-buffered saline +0.05% Tween 20 (TBS-T), and the second was 20% normal swine serum in TBS-T for 15 minutes each. The primary antibody was followed by applying a biotinylated rabbit anti-goat secondary antibody (KP&L; Cat. No. 16-13-06). Signal development was accomplished using a 1:200 dilution of streptavidin-horseradish peroxidase (Invitrogen; Cat. No. 43–4323) for 30 minutes, followed by incubation with Nova Red chromogen solution (Vector; Cat. No. SK-4800). A positive signal was quantified in both bronchioles and alveoli for each tissue section, and a score of 0–4 was assigned according to an integer-based scale of: 0 = no positive alveoli/bronchioles, 1 = 1–10 positive alveoli/bronchioles, 2 = 11–39 positive alveoli/bronchioles, 3 = 40–99 positive alveoli/bronchioles, 4 = >100 positive alveoli/bronchioles. IHC for *Spn* was performed using a rabbit anti-*Streptococcus pneumoniae* polyclonal antibody (Thermo Fisher scientific cat. # PA-7259) followed by biotin-labeled goat anti-rabbit IgG antibody (Thermo Fisher Scientific Cat.#: 65–6140). Five random images were taken for each tissue section that was then analyzed by the quantitative Halo program.

Quantitative reverse transcription polymerase chain reaction (RT-qPCR). BALF and lung tissue homogenates in Trizol were used to assess RSV mRNA expression by RT-qPCR. The assay was performed as published previously in our laboratory [32, 38, 39]. Briefly, RNA isolation from lung tissue and BALF was performed using the TRIzol method followed by

standard DNase treatment. RT-qPCR was carried out using the One-Step Fast qRT-PCR Kit master mix (Quanta, BioScience, Gaithersburg, MD) in a StepOnePlus™ qPCR machine (Applied Biosystems, Carlsbad, CA) in conjunction with PREXCEL-Q assay-optimizing calculations. Primers and probe for RSV M37 nucleoprotein were designed based on RSV accession number M74568. Forward primer: 5′-GCTCTTAGCAAAGTCAAGTTGAACGA; reverse primer: 5′-TGCTCCGTTGGATGGTGTATT; hydrolysis probe: 5′-6FAM-ACACTCAACAAAGATCAAC TTCTGTCATCCAGC-TAMRA.

Additionally, PBMCs were harvested at six days post-RSV infection and added to RNAlater (Sigma) and stored at -80 degrees after an overnight incubation at 4 degrees C. RNA was then isolated by an RNA plus isolation kit (Qiagen, Gaithersburg, MD) per the manufacturer's directions and then subjected to qRT-PCR using a single-step reaction using Luna reagent (NEB, Ipswhich MA). 100mg of frozen lung tissue was also extracted by RNA plus kit per the manufacturer's instructions (Qiagen). The primers and probes (5'-6FAM and Iowa Black Quencher) used were for IL-10, IFNγ, Actin, IL-1β, myeloperoxidase, and IL-17a designed using published lamb cytokine sequences and PrimerDesign (UK) to find optimal pairs. For the detection of changes in gene expression (normalized on Actin), the RNA levels for each were compared with the levels in uninfected lambs (calibrators), and data are presented as the change in expression of each gene. The ΔC_T value for the tissue sample from the calibrator was then subtracted from the ΔC_T value of the corresponding lung tissue of infected mice ($\Delta\Delta C_T$). The increase in cytokine mRNA levels in the infected animals' lung tissue samples compared to tissue samples of baseline (calibrator) animals was then calculated as follows: increase = $2^{\Delta\Delta CT}$.

Hematoxylin-eosin staining and histological scoring of lung sections. Hematoxylin-eosin stained sections were examined via a light microscope. The author MA is a licensed veterinary pathologist and scored each section blinded. An integer-based score of 0–4 was assigned for each parameter (bronchiolitis, syncytial cells, epithelial necrosis, epithelial hyperplasia, alveolar septal thickening, neutrophils in the bronchial lumen, neutrophils in the alveolar lumen, alveolar macrophages, peribronchial lymphocytic infiltration, perivascular lymphocytic infiltration, lymphocytes in alveolar septa, fibrosis), with four as the highest score. A final score was calculated by adding up all measured scores to form a 0–48 score, with 48 as the highest, which is called the accumulative histopathological lesion score. We have used this scoring system in several prior publications [38, 40], although use in *Spn* infected or dually infected lambs was a first for this scoring system. Some of the lambs have larger/bigger normal structures such as the alveolar wall thickness that may be due to the age or the nebulization. Thus, we included these in our score and considered them the minimum score rather than subtracting the score to show zero for the control.

Dual co-localization studies. Hela and Vero cells were infected with RSVA2 (MOI of 0.05) expressing mKate2 fluorescent reporter for 24 hours. Media was washed and replaced with DMEM without antibiotics and labeled *Spn* (serotypes 6c, 19A, and 22F) similar to (Verhoeven et al., 2014) was added for an additional 4 hours at 37 degrees before washing with PBS and fixing using 2% paraformaldehyde. A Zoe fluorescent microscope was used to randomly document both pathogens on the cells in at least ten fields, with all setting similar overlapping the red and green channels on the brightfield.

RSV infection of sheep neutrophils. Sheep neutrophils were obtained by Ficoll gradient centrifugation with removal of PBMCs. Neutrophil/blood pellets were then lysed in ACK lysis for 5 minutes on ice, followed by washing in PBS. Neutrophils were then resuspended in DMEM 10% and infected with RSVa 2001 at MOI of 1 for 4 hours. Neutrophils were then washed three times and held in RNAlater until qRT-PCR for RSV F transcripts could be performed. For confirmation, we derived neutrophils from adult lambs after Percol

centrifugation. We then fixed and permeabilized the neutrophils 4 hours post-infection (MOI of 1 of RSVa 2001 strain) staining with anti-RSV polyclonal antibody (Thermofisher) followed by anti-goat Alexa 555 (Thermofisher). Images were obtained with a ZOE (Biorad, Hercules CA) fluorescent microscope.

Statistical analysis. Statistical analysis used the Wilcoxon signed-rank test for nonparametric and parameters such as accumulative microscopic lesion scoring, followed by nonparametric comparisons for each pair using the Wilcoxon method. One-way ANOVA was followed by all pairs comparison by the Tukey-Kramer HSD method for gross lesion scores and viral titer analyses by RT-qPCR and IFFU assays or by the Kruskal-Wallis test for myeloperoxidase.

Results

Infected lambs replicated RSV and were permissive for *Spn* infection

RSV titers and *Spn* colony-forming units were measured in this study to evaluate the degree of infection by each pathogen and investigate the possible effect(s) of co-infection in the combined RSV-*Spn* group on the replication of each infectious agent. As measured by IFFU, infectious RSV was detected in both RSV and RSV-*Spn* groups. Although not significantly different, RSV titer trended about two-fold higher in the RSV-*Spn* group (Fig 1A). In similarity, we found no significant difference in RSV RNA detected in BALF by RT-qPCR (7.28 and 7.31 viral genomes/ml) (Fig 1B). Furthermore, similar to the IFFU results in lungs, RSV virions measured ex vivo by RT-qPCR in the lung of the RSV-*Spn* group only trended two-fold higher
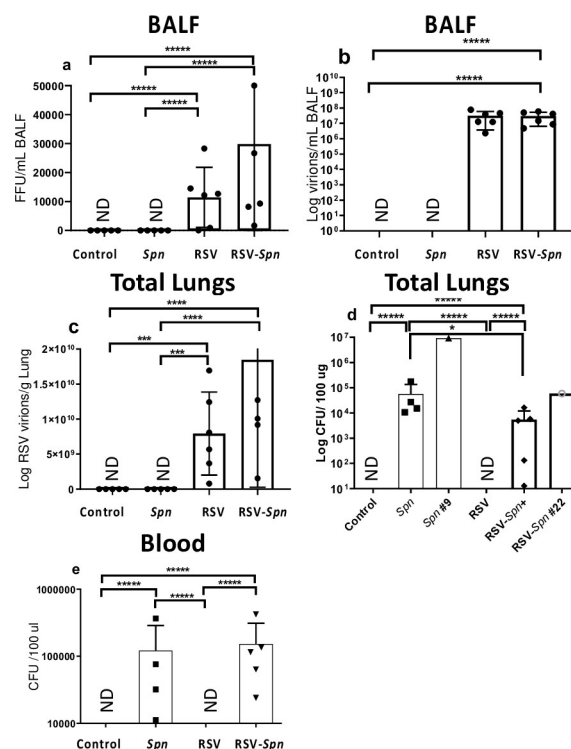

Fig 1. RSV and *Spn* titer in lung tissue and blood. (a) Number of infectious RSV particles as measured by IFFU assay, (b) RSV mRNA level in the BALF, (c) RSV mRNA level in lung tissue (d) *Spn* colony forming unit per 100 μg lung tissue, (e) *Spn* colony forming unit per 100 μl blood, all shown as average + SEM. One animal was not included in the *Spn* group due to death and blood clotting. Animals were either infected with mock media (control), RSV, *Spn*, or RSV followed by *Spn* (RSV-Spn). #11 and #23 died 48 and 36 hrs. after *Spn* inoculation. *P<0.05, **P<0.01, ***P<0.005, **** P<0.001, ***** P<0.0001. LLOD: Lower limit of detection. ND here and all other figures: Not detected.

than the RSV-only group, and again was not significantly different (Fig 1C). While significant differences between groups were not detected with respect to viral burdens, bacterial burdens did exhibit some differences. Specifically, *Spn* was isolated in the lung tissue of both the *Spn* only and the RSV-*Spn* groups with the bacterial titer 8.3-fold higher in the *Spn* only infected group over dually infected (p<0.05) (Fig 1D).

Interestingly, *Spn* titers in lambs that died before the end of the study were the highest of their groups. One lamb in the RSV-*Spn* group humanely euthanized 36 hr. after bacterial inoculation had 59,302 CFU/μg in the lungs, while another lamb in the *Spn only* group euthanized 48 hr after bacterial inoculations had a titer of 9,302,325 CFU/μg (Fig 1D). Both of these animals had much higher bacterial counts, then their group peers, possibly indicating some loss of innate control over the bacteria. While we had hoped for *Spn* being contained only in the lungs, we did detect *Spn* in the blood in both *Spn* infected groups indicating bacteremia/sepsis (Fig 1E) development and possibly indicating a need for further model refinement (i.e., CFU given or alter the route).

Dually infected lambs showed elevated morbidity over *Spn* only

Daily temperatures were taken from each lamb during the study. While uninfected and RSV groups failed to spike a temperature at any point during the infection, *Spn* and RSV-*Spn* groups both exhibited an increase in body temperature after the inoculation of the bacteria indicative of a mild fever as would be typical of *Spn* pneumonia (Fig 2A). However, the differences were not statistically significant, and both had similar temperatures, three days post-inoculation with the bacteria.

Where the two groups did diverge was in the clinical symptom scores. By two days post-*Spn* infection, 3 of the 5 RSV-*Spn* lambs were scored by blinded animal care staff as visibly sick while only 1 of the 5 *Spn* only lambs was scored sick and that animal subsequently died from sepsis that day. The *Spn* alone group was still not scored as showing symptoms by three days post-Spn infection while the RSV-*Spn* lambs all exhibited lethargy, coughing, or wheezing (Fig 2B).
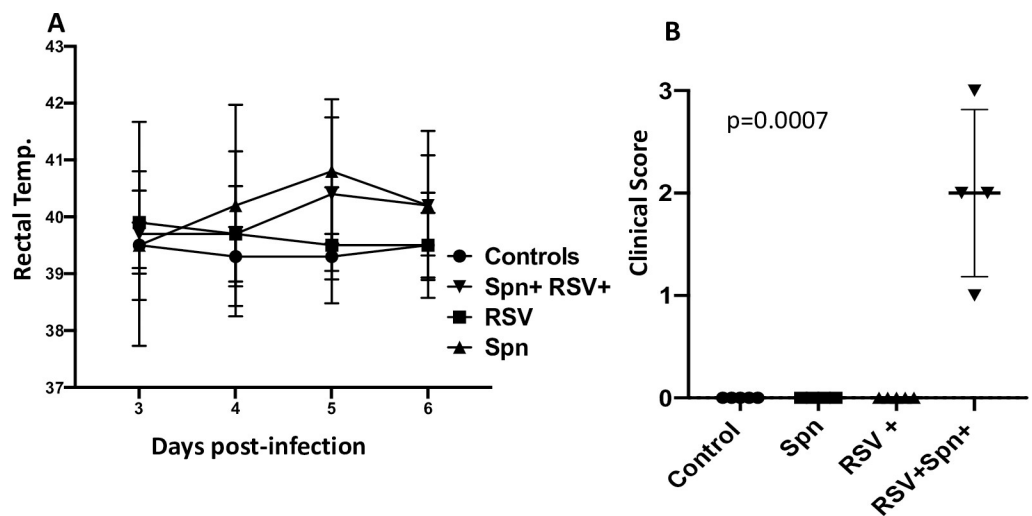

Fig 2. Morbidity levels after infection. (a) Rectal temperatures measured during infection, (b) level of morbidity observed (coughing, wheezing, lethargy, respiratory rate) rated from 1 (least severe) to 5 (most severe) as evaluated by blinded observation of the animals at 6 days post-RSV infection.

RSV and *Spn* induce a well-recognized macroscopic and microscopic lesion

The percent of lung tissue with gross lesions related to either infectious agent was determined at necropsy and with post-necropsy retrospective qualitative analyses. Both RSV and *Spn*-related lesions were found scattered across the lung surface in all lung lobes. Pinpoint dark red areas of lung consolidation characterized RSV lesions. These areas were evident in RSV and RSV-*Spn* groups. There were no differences in the percentage of the lung with RSV macroscopic lesions detected between RSV and RSV-*Spn* groups (Fig 3A and 3C). *Spn* gross lesions are characterized by larger sizes of lung consolidation with bright red color—which was seen to a lesser extent when compared to RSV lesions (Fig 3B and 3D). There was a significant increase (p<0.001) in the percent of gross lesions in the RSV-*Spn* group since it has both RSV associated lesion and *Spn* associated lesion (Fig 3E).

Microscopic lesions observed within the lung tissue reflected the infectious agent used and contradicted our initial expectations (*i.e.*, microscopic lesions caused by RSV infection were multifocal areas of interstitial pneumonia, and bronchiolitis scattered randomly and homogeneously throughout the lung tissue). However, *Spn* induced diffuse homogenous and subtle pathological changes in the lung tissue. Infection with either *Spn*, RSV, or both, markedly increased microscopic lesions (accumulative microscopic lesion score) associated with the disease in comparison to the control group (p<0.05) (Fig 4A–4F). Additionally, the combined RSV-*Spn* infection significantly increased the severity of microscopic lesions in comparison to the *Spn* only group (p<0.05). Lesions varied among lambs, and RSV lesions consisted of thickening of the interalveolar wall with inflammatory cellular infiltrates in the airway adventitia and lamina propria (lymphocytes and plasma cells), the alveolar lumen (alveolar macrophages
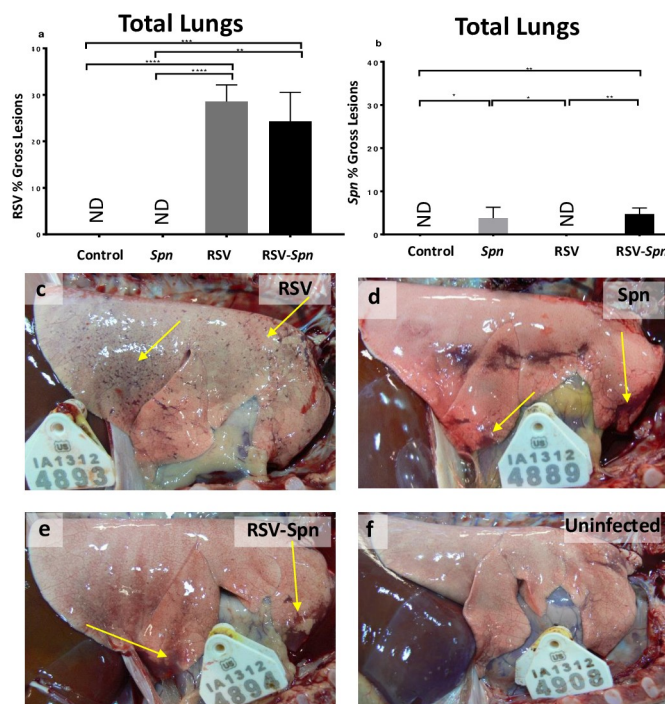

Fig 3. Percent of lung tissue associated with RSV and/or *Spn* infection. Percent of lung tissue associated with RSV lesions (a), *Spn* (b), with photographic representation of RSV-only (c), *Spn*-only (d), RSV-*Spn* (e), or mock infected (f). All show average and SEM. Lambs were either infected with mock media (control), RSV, *Spn*, or RSV followed by *Spn* (*RSV-Spn*). *P<0.05, **P<0.01, ***P<0.005, **** P<0.001, ***** P<0.0001. Arrows show examples of gross lesions.
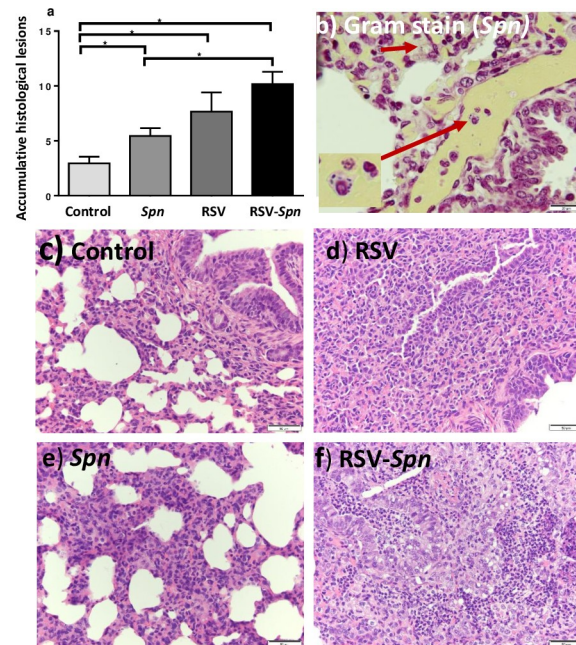
Fig 4. Histologic lesions associated with RSV, *Spn*, and RSV-*Spn* combined infection. (a) Accumulative histologic lesion associated with RSV and *Spn* infection shown as average + SEM (b-f) show a representative photograph of lung tissue sections stained with Gram stain (b), H&E stained tissue section of control (c), RSV only (d), *Spn* only (e), combined *RSV-Spn* (f). Lambs were either infected with mock media (control), RSV, *Spn*, or RSV followed by *Spn* (RSV-*Spn*). * P<0.05, **P<0.01, ***P<0.005, **** P<0.001, ***** P<0.0001.

and neutrophils) (S1 Fig), and bronchiolar lumen (neutrophils), (S2 Fig). With RSV, overall, there was a varying degree of epithelial necrosis and syncytial cell formation (S3 Fig). In comparison, *Spn* lesions consisted of moderate interalveolar wall thickening with inflammatory cellular infiltrate, mainly in the alveolar septae. Most of the microscopic lesions seen with RSV overlapped with *Spn*-induced injury. However, congestion of the interalveolar wall capillaries and hemorrhage was seen only in *Spn*-inoculated lambs.

Immunohistochemistry was used to identify and localize RSV and *Spn* in tissue sections. RSV was present multifocally throughout the sections with bronchial and peribronchial distribution (Fig 5C). Therefore, RSV expression was evaluated in bronchioles and alveoli separately. There were no significant differences between the RSV only and RSV-*Spn* groups in the degree of RSV expression in lung tissue sections (Fig 5A). *Spn* was random and homogenously scattered throughout the lung sections with more intense signals in interalveolar walls and blood capillaries (Fig 5D). Although not significant, there was a 1.5 fold increase in *Spn* staining in the *Spn* only group when compared with the RSV-*Spn* group (Fig 5B).

Divergent cytokine responses occurred between the groups

Next, we examined the cytokine responses in PBMC from lambs at necropsy and found some significant differences in patterns by qRT-PCR between groups (Fig 6A). Using the uninfected controls as the baseline, we found that PBMCs from the RSV only group were positive for IFNγ, IL-1β, while the *Spn* only group were positive for IL-10, IFNγ, and IL-1β. In contrast to both of these groups, RSV-*Spn* lambs were positive (higher than uninfected controls) only for IL-1β. No IL-17a was detected in any of the lambs above uninfected controls, and IL-4 was detected only in the uninfected controls. For additional controls, we tested each cytokine using
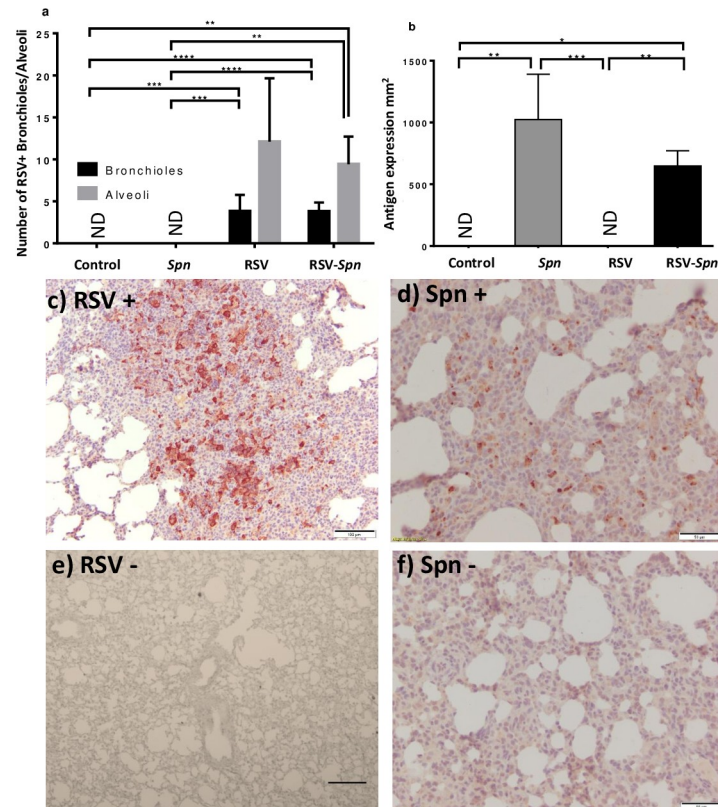
Fig 5. Immunohistochemistry staining of RSV and *Spn* in FFPE lung tissue sections. The number of bronchioles and alveoli express the RSV positive signal (a), surface area (mm^2) occupied by *Spn* IHC positive staining (b), all shown as average + SEM, 5 fields examined. (c) and (d) show a photo representation of RSV (c) and *Spn* (d) IHC positive staining. Uninfected controls were also stained for RSV (e) or *Spn* (f) for comparisons. Animals were either infected with mock media (control), RSV, *Spn*, or RSV followed by *Spn* (RSV-*Spn*). * $P<0.05$, ** $P<0.01$, *** $P<0.005$, **** $P<0.001$, ***** $P<0.0001$.

PMA stimulated PBMCs from adult sheep and detected relative fold changes above unstimulated PBMCs of $>10^{3-8}$ for each cytokine, indicating our detection system was working.

We then tested for myeloperoxidase in extracted lung tissue. We found a significant increase in the amount of myeloperoxidase in the dually infected lambs over all other groups (Fig 6B).

Dual infections in Hela and Vero cells failed to demonstrate enhanced *Spn* attachment to infected cells

Since the literature suggests that Hela cells allow for intact G protein on virions while Vero cells cause a cleavage and the G protein is thought to bind to *Spn* [41–43] directly, we thought to explore these mechanisms since we found many of our *Spn* lesions may not have overlapped with RSV lesions. However, as shown in Fig 7, we failed to observe enhanced RSV and *Spn* dual binding to either Hela or Vero cells suggestive that these two pathogens may not necessarily be interacting as we observed in lung lesions of the lambs. In fact, all three serotypes were tested, while many co-localized with RSV infected cells, appeared to have an equal likelihood of attaching to non-RSV infected cells. Hela and Vero cells made no difference in any of these results.
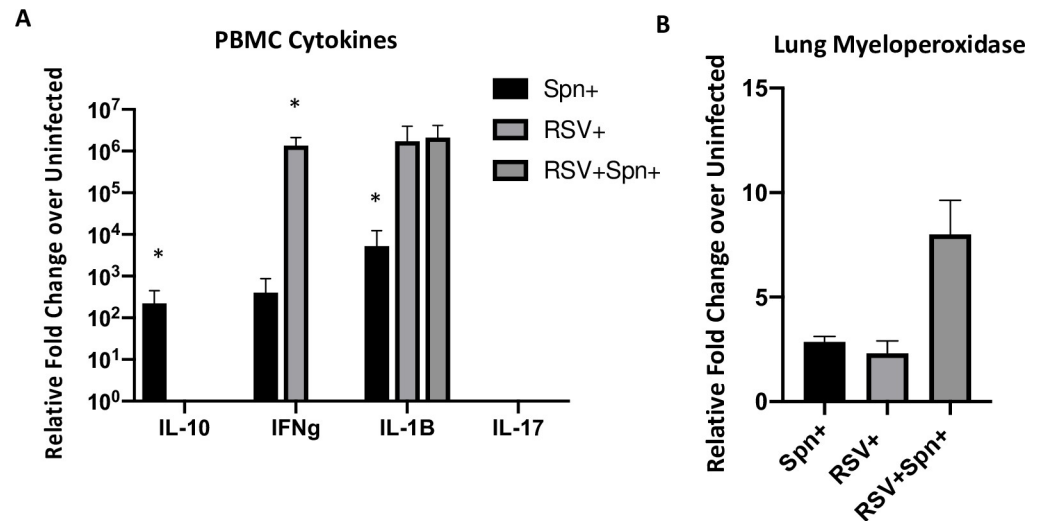
Fig 6. Cytokines responses. (a) qRT-PCR was performed on isolated PBMCs at 6 days post-RSV infection and shown as fold change over uninfected controls. * p<0.05. (b) Myeloperoxidase was determined on lung tissue at 6 days post-infection by qRT-PCR. p = 0.002.

https://doi.org/10.1371/journal.pone.0235026.g006

RSV infection of lamb phagocytes

We next sought to determine whether infection of neutrophils could be occurring in our model and perhaps increasing their pathologic response in the lungs. In prior studies, we found that human infant neutrophils could be infected, and this disrupted their in vitro *Spn* phagocytic activities. Furthermore, infants with severe RSV infections have been observed to have infected blood white blood cells. Thus, we obtained sheep neutrophils and infected them with 1 MOI of RSVa 2001 virus and allowed the infection to occur for 4 hours prior to extensive washing and examination for RSV F transcripts by qRT-PCR. Similar to human neutrophils, we found that sheep neutrophils could be infected with the virus (Fig 8A). In vivo staining for RSV also demonstrated many monocytes/macrophages infected by RSV (Fig 8B), which could also change their activities toward *Spn* in the lungs and also worthy of follow-up studies. As shown in Fig 8C, neutrophils stained positive for viral proteins as well after in vitro infection, further demonstrating that they can be infected.

Discussion

There is a need for additional animal models to study bacterial pneumonia secondary to an initial viral infection in the lung, to study the mechanisms of viral-bacterial co-infection, and to
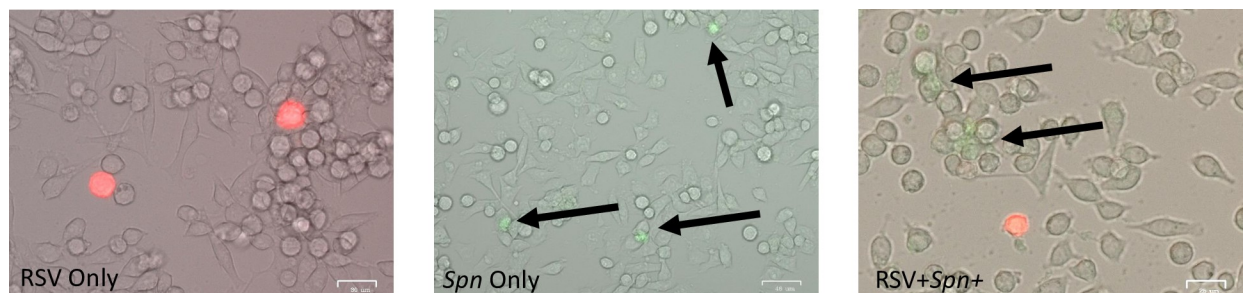

Fig 7. Dual infections of Hela and Vero cells. RSV infection of Hela and Veros proceeded incubation with FITC stained RSV 19A and 22F. Fluorescent microscopy was used to examine for co-localization of both pathogens.

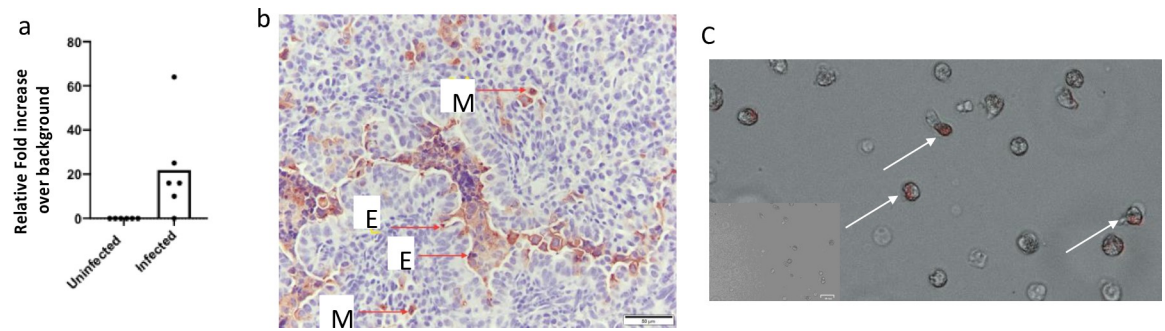https://doi.org/10.1371/journal.pone.0235026.g007

Fig 8. RSV infects phagocytic cells. (a) RSV infection occurs in sheep neutrophils as determined by qRT-PCR after infection of peripheral blood neutrophils in vitro, (b) RSV immunohistochemistry shows many infected monocytes/macrophages in the lungs of infected lambs. E = epithelial cell, M = monocyte/macrophage. (c) Lamb neutrophil infection (post blood harvest) with RSVa 2001 strain 4 hours post infection. Representative of 8 lambs. Arrow indicated infected neutrophil as determined by intracellular staining for total RSV proteins. Inset on C represents a negative stain control for comparison.

evaluate therapeutic interventions. This is particularly true since RSV replicates very poorly in mice. There are significant advantages of using lambs to model RSV infection as a correlate for human infants—including the ability to use human viral strains without adaptation and the similarity of the pathological sequelae [30, 31]. Serotype 22F is thought to have appeared after the introduction of the *S. pneumoniae* vaccine PCV7 ([44]). While this serotype was not widespread in those subsequent years ([44]), 22F is now the second most common serotype causing invasive disease in children less than seven years old and the primary cause in the elderly [45]. Molecular analysis of this serotype also indicates six different lineages and 18% of clinical isolates demonstrating erythromycin resistance ([19]). Thus, this emerging serotype is a component of the PPSV23 vaccine and an important pathogen to observe for in children vaccinated with PCV13.

In this study, we demonstrate that *Spn* readily infects the lungs of lambs and establishes active bacterial pneumonia. A previous study revealed that the peak of RSV titer and infection in lambs is around day three post-viral nebulization, and we used this time-frame to model early human co-infection [38]. This study's results demonstrate consistency in the infection rate of both RSV and *Spn*, as well as an excellent relation to the lesion development induced by either of the infectious agents. We believe that we may also be able to reduce the infection dosage to a lower CFU or potentially use a colonization model to examine co-infection and pneumonia development.

Prior studies in mice and cotton rats with influenza or RSV/*Spn* co-infections demonstrated higher viral loads in dually infected animals [46, 47], although our observed viral (RSV) was not different in this study. Influenza co-infection studies also predict higher *Spn* burdens in the lungs due to damaged epithelial cells serving as anchor points for the opportunistic bacteria. In other studies, RSV with *Spn* in mice or cell culture predicts that the RSV G protein on the infected epithelial surface could also serve as an anchor point for *Spn* in the lungs [41]. However, we did not observe this in infection of either Hela or Vero cells. In contrast to these murine models, we found lower bacterial loads in the co-infection group over the *Spn* only group. These findings suggest that the immune response might control *Spn* in the lungs of lambs better than mice. Importantly, in human clinical studies of co-infection, an increase in nasal colonization numbers of *Spn* upon viral infection has been demonstrated, but this does not translate into higher invasive lung disease [48]. In human studies of high *Spn* colonization, RSV disease appeared less severe [49], suggesting that further using the lamb model to explore mechanistic differences between *Spn* colonization and pneumonia during RSV. Of further

interest, murine studies using IFNγ or IFNγ receptor knockouts and *Spn* infection have shown reduced lung CFUs over wild-type controls with no change in the level of morbidity [50]. Thus, the lower *Spn* counts that we observed in our RSV-*Spn* group could derive from the limited IFNγ response observed in these lambs. Six days post-RSV infection is early for the recruitment of T-cells into the lungs, with three days post-*Spn* also much too early for antibacterial T-cells to infiltrate the lungs. However, peripheral blood could have early trafficking PBMCs migrating between lymph nodes toward the lungs. We are not yet sure why we observed high levels of IFNγ in the RSV group but not the RSV-*Spn* group, but it is feasible that the presence of the bacteria after the virus changed the character of the antiviral T cell response.

The only deaths that occurred in the present study were in the *Spn*-infected groups, and both lambs (lamb 11 in the *Spn* only group, and lamb 23 in the RSV-*Spn* group) had high lung *Spn* colony-forming units/0.1mg tissue. These could represent a failure to control bacterial division and subsequent septicemia.

Lesion severity was consistent with the RSV titer and *Spn* burden as is shown by the significant observed increase in the percent of lung tissue involved by gross lesions, and the increase in the evaluated histological parameters. RSV gross lesions were multifocal lesions scattered randomly in all lung lobes—which is the typical lesion distribution induced by RSV nebulization [32, 38]. However, *Spn* gross lesions' presentation contradicted what was expected by the apparent development of lesions in all lobes—including the caudal lung lobe, which is not typical for bacterial pneumonia in lambs. However, the diffuse bacterial lesions and the presence of *Spn* lesions in the caudal lobe may be due to the inoculation technique used for *Spn* infection. For *Spn* infection, lambs were held vertically by one person and injected intratracheally by the second person leading to a fall of inoculum through the bronchial tree into the caudal lobe, which in this case, was favorable since it gives a bronchopneumonic distribution similar to that found in humans. It is also possible that *Spn* spreads across lung lobes after inoculation either by airflow or vascular flow. RSV-induced microscopic lesions were more prominent in comparison to *Spn*-induced lesions and subsequently led to significant differences between the RSV-*Spn* and *Spn* only groups' accumulative histologic lesion scores. RSV was more prominent in the bronchioles, while *Spn* was diffuse throughout the lung sections.

Although we are still evaluating mechanisms, we believe that the higher morbidity observed in the RSV-*Spn* group may derive from an enhanced neutrophil response found in the lungs. Evidence for this was found in the histopathology and the lower *Spn* burdens in these animals. Likely, RSV infection served as a first activating response to neutrophils that could have then better controlled the secondary bacterial infection. It is also possible that alveolar macrophages were activated by RSV that, in turn, secreted inflammatory mediators that enhance neutrophil activation. Enhanced neutrophil/leukocyte activation contrasts with studies in influenza co-infections in mice–which suggests innate immune exhaustion [51]. While the time of inoculation could be a reason for the observed differences, another could be the small difference between influenza and RSV pathogenesis. In either case, the results suggest further avenues of study using this model. Of interest, morbidity is highest in infants infected with RSV that exhibit significant wheezing [52], and here we observed high wheezing in the presence of dual infection, which further suggests that some of the increased morbidity could be from altered immune responses over the viral only group. There is evidence that RSV can infect neutrophils in humans [52], including our unpublished data. Thus, if dual infection with *Spn* leads to enhanced neutrophil recruitment to the lungs over RSV alone, those cells could become also become infected and have their antiviral or antibacterial responses altered. RSV can lead to alterations in neutrophil interactions with airway epithelium and increase histopathology [53]. Myeloperoxidase is associated with neutrophil release and is known to reduce *Spn* burdens at

the expensive of tissue damage during otitis [54]. RSV is also known to induce neutrophils to release myeloperoxidase and other cytokines [55]. Thus, it would not be surprising if the myeloperoxidase increase observed in the dually infected animals lead to the lower *Spn* burdens are the cost of increased histopathology. Both pathogens at the same may have a strong influence on the level neutrophil degranulation. Thus, the effects of RSV infection on neutrophilic antibacterial responses would be an interesting further study.

Neonates have lower cytokines, including IL-17 [56], compared to older aged individuals due to immunological maturation [57] which is especially compounded during RSV infection as the virus can dramatically alter cytokine patterns [58]. Differences in cytokines could also have played an effect, although we did not test specifically for T cell recall in the lungs that could have differences from the blood. However, we did detect lower IFNγ, IL-β and IL-10 in the *Spn* only group. However, while IFNγ in anti-*Spn* immune studies has not been well studied, one group did find that the cytokine may do very little to reduce *Spn* in the lungs of experimentally infected mice [50]. However, another study found IFNγ did protect mice from *Spn* [59]. In contrast, IFNγ is strongly anti-RSV and capable of significant viral suppression [60]. Another study also found a correlation between lower IL-18 and IFN-γ common in RSV infection and worse *Spn* pneumonia [61]. The limited IFNγ detected here in the dually infected lambs suggest that: (1) IFNγ may do little in lambs for controlling *Spn* since the bacterial counts were only moderately increased and (2) other compensatory mechanisms for a lack of the cytokine and control of viral replication may be occurring. We do not yet know why the dually infected failed to increase their level of IFNγ and think this may warrant further study especially as the role of this key cytokine's control of *Spn*, unlike RSV, is not well known. It is possible that IFNγ is present in the lungs of these lambs as peripheral blood and tissue T cells may not always make the same cytokines. IL-17 however is very important for anti-*Spn* control [62, 63] and a lack of the cytokine has been documented in infants with recurrent acute otitis media with *Spn* [64]. However, it is also known that very young children may make very little IL-17 as compared to older children and adults suggesting that immunological maturation in neonatal lambs may strongly affect their ability to respond to infection [57, 65]. While we cannot comment on contributions of IL-17 mediated protection or lack of in neonates by our study design, we can at least say that a higher amount of Il-17 is likely not contributing to the higher lesions in the dually infected lambs.

In this study, we have developed an animal model of co-infection for RSV and *Spn*. Of course, the study's limitations include low sample numbers in each group that may have limited our ability to achieve some statistical differences in RSV titers. However, prior studies by the authors were adequately powered at these sample numbers. We also emphasize the histologic scoring over the gross lesion scoring since we did not perform morphometry. Future studies will include this assessment. We have determined enhanced disease with co-infection of both pathogens that mirrors studies of human and murine influenza infections, but this may all be due to a complex enhanced inflammatory/immune response to co-infection rather than direct damage by either pathogen alone. While we indicate that changes in neutrophil recruitment or their function may be occurring, we did not specifically focus as much attention on this, such as dissection of differences in chemokine in the lungs that draw these cells into the lungs or how RSV actually might modify their activity since this was found after the study completed. Although murine studies certainly have their place for modeling infections, their poor replication of RSV, consistent development of sepsis with *Spn* experimental infections, and rapid aging (days in mice versus months in lambs) makes studying dual infections in very young animals as surrogates for human infants or neonates hard. Further studies in the lamb model, which is not without its limitations, with attention to further dissecting the potential mechanisms identified here are certainly warranted. Furthermore, additional studies will

allow refinement of this model and will include variations in inoculum volume/concentration, lung versus nasal instillation, the time between infections, and kinetic analyses.

Supporting information

S1 Fig. Severe diffuse congestion and dilation of the blood capillaries in the alveolar wall. Representative photo of this pathology from *Spn* only group. This was seen mostly in the *Spn* -only infected group.
(TIF)

S2 Fig. Higher magnification with focal area of alveolar wall thickening by lymphocytes. Representative photo of this pathology from RSV only group.
(TIF)

S3 Fig. Intense neutrophil infiltration in the RSV-*Spn* co-infected group in comparison to the control and groups solely infected with either RSV or *Spn*. Representative photos of each group looking for neutrophils where large clusters of neutrophils (yellow arrows pointing to neutrophil clusters) were only found in the dual infection group.
(TIF)

Author Contributions

Conceptualization: Mark Ackermann, David Verhoeven.

Data curation: Sarhad Alnajjar, Panchan Sitthicharoenchai, Jack Gallup, Mark Ackermann.

Funding acquisition: David Verhoeven.

Investigation: Sarhad Alnajjar, Panchan Sitthicharoenchai, Mark Ackermann, David Verhoeven.

Project administration: David Verhoeven.

Supervision: David Verhoeven.

Writing – original draft: Sarhad Alnajjar.

Writing – review & editing: Mark Ackermann, David Verhoeven.

References

1. Nair H, Nokes DJ, Gessner BD, Dherani M, Madhi SA, Singleton RJ, et al. Global burden of acute lower respiratory infections due to respiratory syncytial virus in young children: a systematic review and meta-analysis. Lancet. 2010; 375(9725):1545–55. https://doi.org/10.1016/S0140-6736(10)60206-1 PMID: 20399493; PubMed Central PMCID: PMC2864404.

2. Glezen WP, Taber LH, Frank AL, Kasel JA. Risk of primary infection and reinfection with respiratory syncytial virus. Am J Dis Child. 1986; 140(6):543–6. https://doi.org/10.1001/archpedi.1986.02140200053026 PMID: 3706232.

3. Kwon YS, Park SH, Kim MA, Kim HJ, Park JS, Lee MY, et al. Risk of mortality associated with respiratory syncytial virus and influenza infection in adults. BMC Infect Dis. 2017; 17(1):785. https://doi.org/10.1186/s12879-017-2897-4 PMID: 29262784; PubMed Central PMCID: PMC5738863.

4. Thorburn K, Harigopal S, Reddy V, Taylor N, van Saene HK. High incidence of pulmonary bacterial co-infection in children with severe respiratory syncytial virus (RSV) bronchiolitis. Thorax. 2006; 61 (7):611–5. https://doi.org/10.1136/thx.2005.048397 PMID: 16537670; PubMed Central PMCID: PMC2104657.

5. Madhi SA, Klugman KP, Vaccine Trialist G. A role for Streptococcus pneumoniae in virus-associated pneumonia. Nat Med. 2004; 10(8):811–3. https://doi.org/10.1038/nm1077 PMID: 15247911; PubMed Central PMCID: PMC7095883.

6. Verhoeven D, Xu Q, Pichichero ME. Differential impact of respiratory syncytial virus and parainfluenza virus on the frequency of acute otitis media is explained by lower adaptive and innate immune responses in otitis-prone children. Clin Infect Dis. 2014; 59(3):376–83. https://doi.org/10.1093/cid/ciu303 PMID: 24785236; PubMed Central PMCID: PMC4155442.

7. Madhi SA, Schoub B, Simmank K, Blackburn N, Klugman KP. Increased burden of respiratory viral associated severe lower respiratory tract infections in children infected with human immunodeficiency virus type-1. J Pediatr. 2000; 137(1):78–84. https://doi.org/10.1067/mpd.2000.105350 PMID: 10891826.

8. Weinberger DM, Grant LR, Steiner CA, Weatherholtz R, Santosham M, Viboud C, et al. Seasonal drivers of pneumococcal disease incidence: impact of bacterial carriage and viral activity. Clin Infect Dis. 2014; 58(2):188–94. https://doi.org/10.1093/cid/cit721 PMID: 24190895; PubMed Central PMCID: PMC3871795.

9. Weinberger DM, Klugman KP, Steiner CA, Simonsen L, Viboud C. Association between respiratory syncytial virus activity and pneumococcal disease in infants: a time series analysis of US hospitalization data. PLoS Med. 2015; 12(1):e1001776. https://doi.org/10.1371/journal.pmed.1001776 PMID: 25562317; PubMed Central PMCID: PMC4285401.

10. Zhou H, Haber M, Ray S, Farley MM, Panozzo CA, Klugman KP. Invasive pneumococcal pneumonia and respiratory virus co-infections. Emerg Infect Dis. 2012; 18(2):294–7. https://doi.org/10.3201/eid1802.102025 PMID: 22305270; PubMed Central PMCID: PMC3310442.

11. Watson M, Gilmour R, Menzies R, Ferson M, McIntyre P, New South Wales Pneumococcal N. The association of respiratory viruses, temperature, and other climatic parameters with the incidence of invasive pneumococcal disease in Sydney, Australia. Clin Infect Dis. 2006; 42(2):211–5. https://doi.org/10.1086/498897 PMID: 16355331.

12. Griffiths C, Drews SJ, Marchant DJ. Respiratory Syncytial Virus: Infection, Detection, and New Options for Prevention and Treatment. Clin Microbiol Rev. 2017; 30(1):277–319. https://doi.org/10.1128/CMR.00010-16 PMID: 27903593; PubMed Central PMCID: PMC5217795.

13. Jain S, Williams DJ, Arnold SR, Ampofo K, Bramley AM, Reed C, et al. Community-acquired pneumonia requiring hospitalization among U.S. children. N Engl J Med. 2015; 372(9):835–45. https://doi.org/10.1056/NEJMoa1405870 PMID: 25714161; PubMed Central PMCID: PMC4697461.

14. Michelow IC, Olsen K, Lozano J, Rollins NK, Duffy LB, Ziegler T, et al. Epidemiology and clinical characteristics of community-acquired pneumonia in hospitalized children. Pediatrics. 2004; 113(4):701–7. https://doi.org/10.1542/peds.113.4.701 PMID: 15060215.

15. Weiser JN, Ferreira DM, Paton JC. Streptococcus pneumoniae: transmission, colonization and invasion. Nat Rev Microbiol. 2018; 16(6):355–67. https://doi.org/10.1038/s41579-018-0001-8 PMID: 29599457; PubMed Central PMCID: PMC5949087.

16. Bogaert D, De Groot R, Hermans PW. Streptococcus pneumoniae colonisation: the key to pneumococcal disease. Lancet Infect Dis. 2004; 4(3):144–54. https://doi.org/10.1016/S1473-3099(04)00938-7 PMID: 14998500.

17. O'Brien KL, Wolfson LJ, Watt JP, Henkle E, Deloria-Knoll M, McCall N, et al. Burden of disease caused by Streptococcus pneumoniae in children younger than 5 years: global estimates. Lancet. 2009; 374 (9693):893–902. https://doi.org/10.1016/S0140-6736(09)61204-6 PMID: 19748398.

18. Klugman KP, Madhi SA, Huebner RE, Kohberger R, Mbelle N, Pierce N, et al. A trial of a 9-valent pneumococcal conjugate vaccine in children with and those without HIV infection. N Engl J Med. 2003; 349 (14):1341–8. https://doi.org/10.1056/NEJMoa035060 PMID: 14523142.

19. Demczuk WHB, Martin I, Hoang L, Van Caeseele P, Lefebvre B, Horsman G, et al. Phylogenetic analysis of emergent Streptococcus pneumoniae serotype 22F causing invasive pneumococcal disease using whole genome sequencing. PLoS One. 2017; 12(5):e0178040. https://doi.org/10.1371/journal.pone.0178040 PMID: 28531208; PubMed Central PMCID: PMC5439729.

20. Brealey JC, Chappell KJ, Galbraith S, Fantino E, Gaydon J, Tozer S, et al. Streptococcus pneumoniae colonization of the nasopharynx is associated with increased severity during respiratory syncytial virus infection in young children. Respirology. 2018; 23(2):220–7. https://doi.org/10.1111/resp.13179 PMID: 28913912.

21. MacIntyre CR, Chughtai AA, Barnes M, Ridda I, Seale H, Toms R, et al. The role of pneumonia and secondary bacterial infection in fatal and serious outcomes of pandemic influenza a(H1N1)pdm09. BMC Infect Dis. 2018; 18(1):637. https://doi.org/10.1186/s12879-018-3548-0 PMID: 30526505; PubMed Central PMCID: PMC6286525.

22. Rudd JM, Ashar HK, Chow VT, Teluguakula N. Lethal Synergism between Influenza and Streptococcus pneumoniae. J Infect Pulm Dis. 2016; 2(2). https://doi.org/10.16966/2470-3176.114 PMID: 27981251; PubMed Central PMCID: PMC5154682.

23. Taylor G. Animal models of respiratory syncytial virus infection. Vaccine. 2017; 35(3):469–80. https://doi.org/10.1016/j.vaccine.2016.11.054 PMID: 27908639; PubMed Central PMCID: PMC5244256.

24. Bem RA, Domachowske JB, Rosenberg HF. Animal models of human respiratory syncytial virus disease. Am J Physiol Lung Cell Mol Physiol. 2011; 301(2):L148–56. https://doi.org/10.1152/ajplung.00065.2011 PMID: 21571908; PubMed Central PMCID: PMC3154630.

25. Altamirano-Lagos MJ, Diaz FE, Mansilla MA, Rivera-Perez D, Soto D, McGill JL, et al. Current Animal Models for Understanding the Pathology Caused by the Respiratory Syncytial Virus. Front Microbiol. 2019; 10:873. https://doi.org/10.3389/fmicb.2019.00873 PMID: 31130923; PubMed Central PMCID: PMC6510261.

26. Jacobs MR, Good CE, Bajaksouzian S, Windau AR. Emergence of Streptococcus pneumoniae serotypes 19A, 6C, and 22F and serogroup 15 in Cleveland, Ohio, in relation to introduction of the protein-conjugated pneumococcal vaccine. Clin Infect Dis. 2008; 47(11):1388–95. https://doi.org/10.1086/592972 PMID: 18959493.

27. Berman-Rosa M, O'Donnell S, Barker M, Quach C. Efficacy and Effectiveness of the PCV-10 and PCV-13 Vaccines Against Invasive Pneumococcal Disease. Pediatrics. 2020; 145(4). https://doi.org/10.1542/peds.2019-0377 PMID: 32156773.

28. Balsells E, Guillot L, Nair H, Kyaw MH. Serotype distribution of Streptococcus pneumoniae causing invasive disease in children in the post-PCV era: A systematic review and meta-analysis. PLoS One. 2017; 12(5):e0177113. https://doi.org/10.1371/journal.pone.0177113 PMID: 28486544; PubMed Central PMCID: PMC5423631.

29. Roymans D, Alnajjar SS, Battles MB, Sitthicharoenchai P, Furmanova-Hollenstein P, Rigaux P, et al. Therapeutic efficacy of a respiratory syncytial virus fusion inhibitor. Nat Commun. 2017; 8(1):167. https://doi.org/10.1038/s41467-017-00170-x PMID: 28761099; PubMed Central PMCID: PMC5537225.

30. Ackermann MR. Lamb model of respiratory syncytial virus-associated lung disease: insights to pathogenesis and novel treatments. ILAR J. 2014; 55(1):4–15. https://doi.org/10.1093/ilar/ilu003 PMID: 24936027; PubMed Central PMCID: PMC4158344.

31. Derscheid RJ, Ackermann MR. Perinatal lamb model of respiratory syncytial virus (RSV) infection. Viruses. 2012; 4(10):2359–78. https://doi.org/10.3390/v4102359 PMID: 23202468; PubMed Central PMCID: PMC3497056.

32. Derscheid RJ, van Geelen A, McGill JL, Gallup JM, Cihlar T, Sacco RE, et al. Human respiratory syncytial virus Memphis 37 grown in HEp-2 cells causes more severe disease in lambs than virus grown in Vero cells. Viruses. 2013; 5(11):2881–97. https://doi.org/10.3390/v5112881 PMID: 24284879; PubMed Central PMCID: PMC3856420.

33. Garedew L AG, Yilma R, Zeleke A, Gelaye E. Isolation of diverse bacterial species associated with maedi-visna infection of sheep in Ethiopia. Afr J Microbiol Res. 2010; 4:014–21.

34. Zaghawa A HH, El-Sify A. Epidemiological and clinical studies on respiratory affections of sheep. Minufiya Vet J. 2010; 7:93–103.

35. DeVincenzo JP, Wilkinson T, Vaishnaw A, Cehelsky J, Meyers R, Nochur S, et al. Viral load drives disease in humans experimentally infected with respiratory syncytial virus. Am J Respir Crit Care Med. 2010; 182(10):1305–14. https://doi.org/10.1164/rccm.201002-0221OC PMID: 20622030; PubMed Central PMCID: PMC3001267.

36. Kim YI, DeVincenzo JP, Jones BG, Rudraraju R, Harrison L, Meyers R, et al. Respiratory syncytial virus human experimental infection model: provenance, production, and sequence of low-passaged memphis-37 challenge virus. PLoS One. 2014; 9(11):e113100. https://doi.org/10.1371/journal.pone.0113100 PMID: 25415360; PubMed Central PMCID: PMC4240712.

37. Grosz DD, van Geelen A, Gallup JM, Hostetter SJ, Derscheid RJ, Ackermann MR. Sucrose stabilization of Respiratory Syncytial Virus (RSV) during nebulization and experimental infection. BMC Res Notes. 2014; 7:158. https://doi.org/10.1186/1756-0500-7-158 PMID: 24642084; PubMed Central PMCID: PMC3995326.

38. Larios Mora A, Detalle L, Van Geelen A, Davis MS, Stohr T, Gallup JM, et al. Kinetics of Respiratory Syncytial Virus (RSV) Memphis Strain 37 (M37) Infection in the Respiratory Tract of Newborn Lambs as an RSV Infection Model for Human Infants. PLoS One. 2015; 10(12):e0143580. https://doi.org/10.1371/journal.pone.0143580 PMID: 26641081; PubMed Central PMCID: PMC4671688.

39. Derscheid RJ, Gallup JM, Knudson CJ, Varga SM, Grosz DD, van Geelen A, et al. Effects of formalin-inactivated respiratory syncytial virus (FI-RSV) in the perinatal lamb model of RSV. PLoS One. 2013; 8(12):e81472. https://doi.org/10.1371/journal.pone.0081472 PMID: 24324695; PubMed Central PMCID: PMC3855688.

40. Larios Mora A, Detalle L, Gallup JM, Van Geelen A, Stohr T, Duprez L, et al. Delivery of ALX-0171 by inhalation greatly reduces respiratory syncytial virus disease in newborn lambs. MAbs. 2018; 10(5):778–95. https://doi.org/10.1080/19420862.2018.1470727 PMID: 29733750; PubMed Central PMCID: PMC6150622.

41. Avadhanula V, Wang Y, Portner A, Adderson E. Nontypeable Haemophilus influenzae and Streptococcus pneumoniae bind respiratory syncytial virus glycoprotein. J Med Microbiol. 2007; 56(Pt 9):1133–7. https://doi.org/10.1099/jmm.0.47086-0 PMID: 17761473.

42. Hament JM, Aerts PC, Fleer A, Van Dijk H, Harmsen T, Kimpen JL, et al. Enhanced adherence of Streptococcus pneumoniae to human epithelial cells infected with respiratory syncytial virus. Pediatr Res. 2004; 55(6):972–8. https://doi.org/10.1203/01.PDR.0000127431.11750.D9 PMID: 15103015.

43. Smith CM, Sandrini S, Datta S, Freestone P, Shafeeq S, Radhakrishnan P, et al. Respiratory syncytial virus increases the virulence of Streptococcus pneumoniae by binding to penicillin binding protein 1a. A new paradigm in respiratory infection. Am J Respir Crit Care Med. 2014; 190(2):196–207. https://doi.org/10.1164/rccm.201311-2110OC PMID: 24941423; PubMed Central PMCID: PMC4226051.

44. Carnalla-Barajas MN, Soto-Nogueron A, Sanchez-Aleman MA, Solorzano-Santos F, Velazquez-Meza ME, Echaniz-Aviles G, et al. Changing trends in serotypes of S. pneumoniae isolates causing invasive and non-invasive diseases in unvaccinated population in Mexico (2000–2014). Int J Infect Dis. 2017; 58:1–7. https://doi.org/10.1016/j.ijid.2017.02.005 PMID: 28216181.

45. Cui YA, Patel H, O'Neil WM, Li S, Saddier P. Pneumococcal serotype distribution: A snapshot of recent data in pediatric and adult populations around the world. Hum Vaccin Immunother. 2017; 13(6):1–13. https://doi.org/10.1080/21645515.2016.1277300 PMID: 28125317; PubMed Central PMCID: PMC5489298.

46. Smith AM, Adler FR, Ribeiro RM, Gutenkunst RN, McAuley JL, McCullers JA, et al. Kinetics of coinfection with influenza A virus and Streptococcus pneumoniae. PLoS Pathog. 2013; 9(3):e1003238. https://doi.org/10.1371/journal.ppat.1003238 PMID: 23555251; PubMed Central PMCID: PMC3605146.

47. Nguyen DT, Louwen R, Elberse K, van Amerongen G, Yuksel S, Luijendijk A, et al. Streptococcus pneumoniae Enhances Human Respiratory Syncytial Virus Infection In Vitro and In Vivo. PLoS One. 2015; 10(5):e0127098. https://doi.org/10.1371/journal.pone.0127098 PMID: 25970287; PubMed Central PMCID: PMC4430531.

48. Moyes J, Cohen C, Pretorius M, Groome M, von Gottberg A, Wolter N, et al. Epidemiology of respiratory syncytial virus-associated acute lower respiratory tract infection hospitalizations among HIV-infected and HIV-uninfected South African children, 2010–2011. J Infect Dis. 2013; 208 Suppl 3:S217–26. https://doi.org/10.1093/infdis/jit479 PMID: 24265481.

49. Vissers M, Ahout IM, van den Kieboom CH, van der Gaast-de Jongh CE, Groh L, Cremers AJ, et al. High pneumococcal density correlates with more mucosal inflammation and reduced respiratory syncytial virus disease severity in infants. BMC Infect Dis. 2016; 16:129. https://doi.org/10.1186/s12879-016-1454-x PMID: 26983753; PubMed Central PMCID: PMC4794819.

50. Rijneveld AW, Lauw FN, Schultz MJ, Florquin S, Te Velde AA, Speelman P, et al. The role of interferon-gamma in murine pneumococcal pneumonia. J Infect Dis. 2002; 185(1):91–7. https://doi.org/10.1086/338122 PMID: 11756986.

51. McNamee LA, Harmsen AG. Both influenza-induced neutrophil dysfunction and neutrophil-independent mechanisms contribute to increased susceptibility to a secondary Streptococcus pneumoniae infection. Infect Immun. 2006; 74(12):6707–21. https://doi.org/10.1128/IAI.00789-06 PMID: 16982840; PubMed Central PMCID: PMC1698099.

52. Halfhide CP, Flanagan BF, Brearey SP, Hunt JA, Fonceca AM, McNamara PS, et al. Respiratory syncytial virus binds and undergoes transcription in neutrophils from the blood and airways of infants with severe bronchiolitis. J Infect Dis. 2011; 204(3):451–8. https://doi.org/10.1093/infdis/jir280 PMID: 21742845; PubMed Central PMCID: PMC3132143.

53. Yu Deng JAH, Robinson Elisabeth, Ren Luo, Smyth Rosalind L., Smith Claire M.. Neutrophil-Airway Epithelial Interactions Result in Increased Epithelial Damage and Viral Clearance during Respiratory Syncytial Virus Infection. Journal of Virology. 2020; 94(13):e02161–19. https://doi.org/10.1128/JVI.02161-19 PMID: 32295918

54. Yun Xiang CJ, Wang Wei, Wang Zimeng, Huang Yifei, Fan Fangmei, Ma Yurong, et al. The critical role of myeloperoxidase in Streptococcus pneumoniae clearance and tissue damage during mouse acute otitis media. Innate Immunology. 2017; 23(3):296–306. https://doi.org/10.1177/1753425917693907 PMID: 28359218

55. P Jaovisidha MEP, Brees A A, Carpenter L R, Moy J N. Respiratory syncytial virus stimulates neutrophil degranulation and chemokine release. Journal of Immunology 1999; 163(5):2816–20.

56. Styze de Roock AS, Scholman Rianne, Hoeks Sanne BEA, Meerding Jenny, Prakken Berent, Boes Marianne. Defective TH17 development in human neona- tal T cells involves reduced RORC2 mRNA content. J Allergy Clin Immunol. 2013. https://doi.org/10.1016/j.jaci.2013.04.014 PMID: 23726039

57. Verhoeven D. Influence of Immunological Maturity on Respiratory Syncytial Virus-Induced Morbidity in Young Children. Viral Immunol. 2019; 32(2):76–83. https://doi.org/10.1089/vim.2018.0121 PMID: 30499759.

58. ABERLE SWA J H, REBHANDL W, PRACHER E, KUNDI M, and POPOW-KRAUPP T. Decreased interferon-gamma response in respiratory syncytial virus compared to other respiratory viral infections in infants. Clinical and Experimental Immunology. 2004; 137(1):146–50. https://doi.org/10.1111/j.1365-2249.2004.02504.x PMID: 15196255

59. Rubins JB, Pomeroy C. Role of gamma interferon in the pathogenesis of bacteremic pneumococcal pneumonia. Infect Immun. 1997; 65(7):2975–7. https://doi.org/10.1128/IAI.65.7.2975-2977.1997 PMID: 9199475; PubMed Central PMCID: PMC175417.

60. van Schaik SM, Obot N, Enhorning G, Hintz K, Gross K, Hancock GE, et al. Role of interferon gamma in the pathogenesis of primary respiratory syncytial virus infection in BALB/c mice. J Med Virol. 2000; 62 (2):257–66. https://doi.org/10.1002/1096-9071(200010)62:2<257::aid-jmv19>3.0.co;2-m PMID: 11002257.

61. Takehiko Shibata AM, Ogata Ruiko,3 Nakamura Shigeki,Ito Toshihiro, Nagata Kisaburo, Terauchi Yoshihiko,et al. Respiratory syncytial virus infection exacerbates pneumococcal pneumonia via Gas6/Axl-mediated macrophage polarization. Journal of Clinical Investigation. 2020; 130(6):3021–37. https://doi.org/10.1172/JCI125505 PMID: 32364537

62. Moffitt KL, Gierahn TM, Lu YJ, Gouveia P, Alderson M, Flechtner JB, et al. T(H)17-based vaccine design for prevention of Streptococcus pneumoniae colonization. Cell Host Microbe. 9(2):158–65. https://doi.org/10.1016/j.chom.2011.01.007 PMID: 21320698.

63. Lu YJ, Gross J, Bogaert D, Finn A, Bagrade L, Zhang Q, et al. Interleukin-17A mediates acquired immunity to pneumococcal colonization. PLoS Pathog. 2008; 4(9):e1000159. https://doi.org/10.1371/journal.ppat.1000159 PMID: 18802458

64. Basha S, Kaur R, Mosmann TR, Pichichero ME. Reduced T-Helper 17 Responses to Streptococcus pneumoniae in Infection-Prone Children Can Be Rescued by Addition of Innate Cytokines. J Infect Dis. 2017; 215(8):1321–30. https://doi.org/10.1093/infdis/jix090 PMID: 28201637; PubMed Central PMCID: PMC5441110.

65. Verhoeven D. Immunometabolism and innate immunity in the context of immunological maturation and respiratory pathogens in young children. J Leukoc Biol. 2019; 106(2):301–8. https://doi.org/10.1002/JLB.MR0518-204RR PMID: 30605225.